ARL-TR-8182 ● OCT 2017

US Army Research Laboratory

Plasmonic and Magnetically Responsive Gold Shell–Magnetic Nanorod Hybrids

by Mackenzie G Williams, Devon A Boyne, Ngon Tran, Andres A Bujanda, and Mark H Griep

NOTICES

Disclaimers

ARL-TR-8182 ● OCT 2017

US Army Research Laboratory

Plasmonic and Magnetically Responsive Gold Shell–Magnetic Nanorod Hybrids

by Mackenzie G Williams, Devon A Boyne, and Ngon Tran
Oak Ridge Institute for Science and Education (ORISE)

Andres A Bujanda and Mark H Griep
Weapons and Materials Research Directorate, ARL

REPORT DOCUMENTATION PAGE	*Form Approved OMB No. 0704-0188*

1. REPORT DATE *(DD-MM-YYYY)*	2. REPORT TYPE	3. DATES COVERED (From - To)
October 2017	Technical Report	June 2016–December 2016

4. TITLE AND SUBTITLE	5a. CONTRACT NUMBER
Plasmonic and Magnetically Responsive Gold Shell–Magnetic Nanorod Hybrids	
	5b. GRANT NUMBER
	5c. PROGRAM ELEMENT NUMBER
6. AUTHOR(S)	5d. PROJECT NUMBER
Mackenzie G Williams, Devon A Boyne, Ngon Tran, Andres A Bujanda, and Mark H Griep	
	5e. TASK NUMBER
	5f. WORK UNIT NUMBER
7. PERFORMING ORGANIZATION NAME(S) AND ADDRESS(ES)	8. PERFORMING ORGANIZATION REPORT NUMBER
US Army Research Laboratory ATTN: RDRL-WMM-A Aberdeen Proving Ground, MD 21005-5069	ARL-TR-8182
9. SPONSORING/MONITORING AGENCY NAME(S) AND ADDRESS(ES)	10. SPONSOR/MONITOR'S ACRONYM(S)
	11. SPONSOR/MONITOR'S REPORT NUMBER(S)

12. DISTRIBUTION/AVAILABILITY STATEMENT

Approved for public release; distribution is unlimited.

13. SUPPLEMENTARY NOTES

14. ABSTRACT

In this work we demonstrated a new methodology to create asymmetric magnetic nanorods with a plasmonically active gold outer shell. The multistage approach involves the synthesis of a precursor iron (III) oxide-hydroxide (FeOOH) nanorod, where the incorporation of a protective silica (SiO_2) shell allows for the material/morphology to survive hydrothermal treatment and subsequent transition to magnetically responsive iron (II, III) oxide (Fe_3O_4). On the magnetic nanorod–SiO_2 particle, a thin gold layer is grown to directly introduce tailorable plasmonic properties. This approach is demonstrated applicable to both spherical and asymmetric morphologies, allowing the hybrid materials to be readily engineered for precise magnetic and plasmonic responses.

15. SUBJECT TERMS

magnetic nanorods, gold nanoshell, plasmonics, nano-additives, core-shell

16. SECURITY CLASSIFICATION OF:			17. LIMITATION OF ABSTRACT	18. NUMBER OF PAGES	19a. NAME OF RESPONSIBLE PERSON
					Mark H Griep
a. REPORT	b. ABSTRACT	c. THIS PAGE	SAR	26	19b. TELEPHONE NUMBER (Include area code)
Unclassified	Unclassified	Unclassified			410-306-4953

Standard Form 298 (Rev. 8/98)
Prescribed by ANSI Std. Z39.18

Contents

List of Figures

Acknowledgments

This research was supported in part by an appointment to the Postgraduate Research Participation Program at the US Army Research Laboratory (ARL) administered by the Oak Ridge Institute for Science and Education through an interagency agreement between the US Department of Energy and ARL.

INTENTIONALLY LEFT BLANK.

1. Introduction

Multifunctional nanomaterials have emerged as enabling technologies toward a diverse array of applications including bio-targeting/sensing,[1,2] structural enhancement/health monitoring,[3,4] and energy harvesting/storage.[5,6] Typical approaches to achieve tailored multifunctionality include the hybridization of separate materials classes, each adding a unique functional attribute to the final composite. Certain material designs, such as plasmonic and magnetic nanomaterials, however, can independently enable multifunctional platforms through tailored design and implementation of the engineered materials.

Plasmonic nanomaterials, for example, have demonstrated functionalities including tunable light absorption,[7,8] photothermal heating,[9] biosensing,[10] contrast marker,[11] drug carrier,[12] and directed electron transfer[13]—all achieved with the same material composition/morphology. This multifunctionality is enabled by the generated plasmon oscillations resulting from absorbed resonant light radiation, with diverse functionalities resulting from tailored interactions with the plasmon field. Likewise, magnetic nanomaterials have independently been tailored toward multiple application areas including material separation,[14] in vivo cellular targeting,[15] ablation therapy,[16] drug delivery,[17] imaging,[18] and sensors.[19]

With the multitude of material functions enabled independently by these material classes, approaches to hybridize plasmonic/magnetic nanomaterials could enable new technological opportunities. Recent efforts have demonstrated successful hybridization approaches included planar layering, intermixed particles,[20,21] and core-shell structures.[22,23] For nano-additive material designs, hybrid plasmonic/magnetic particles have been limited to spherical core-shell designs,[22,24] which limits plasmonic tunability parameters enabled by asymmetric morphologies. Through this work, methodologies are developed to create asymmetric nanorod morphologies composed of an iron (II, III) oxide (Fe_3O_4) magnetic core with a plasmonically active gold (Au) outer shell.

2. Experimental Procedure

2.1 Materials

All chemicals were purchased from Sigma-Aldrich (St. Louis, Missouri) and solutions prepared were aqueous, unless otherwise noted:

- Fe_3O_4 nanospheres (10 nm)
- cetyltrimethylammonium bromide (CTAB)

- sodium hydroxide (NaOH)
- tetraethoxy orthosilicate (TEOS)
- methanol
- ethanol
- isopropanol
- ammonium hydroxide
- (3-aminopropyl)triethoxysilane (APTES)
- formaldehyde solution
- L-glutathione
- trisodium citrate
- tetrakis(hydroxymethyl)phosphonium chloride (THPC)
- chloroauric acid
- potassium carbonate
- hydrochloric acid
- iron (III) chloride hexahydrate ($FeCl_3$•$6H_2O$)
- polyacrylic acid sodium salt (PAA)
- ethylene glycol
- diethylene glycol
- iron (III) acetylacetonate ($Fe(acac)_3$)
- 1,2-hexadecanediol
- oleic acid
- oleylamine
- benzyl ether
- Igepal-CO520
- hexanes
- Millipore (18 ohms) water

2.2 Synthesis

2.2.1 Stock Solutions

The seed and plating solutions were prepared ahead of time and kept refrigerated to age for several days before use. To make the THPC seed solution, 32 mL of NaOH (0.1 M) was added to 307.2 mL water and the solution was well mixed. Trisodium citrate (68 mM, 24 mL) and THPC (85 mM, 8 mL) were added and the mixture was shaken well for a minimum of 10 min. Chloroauric acid ($HAuCl_4$) (25 mM, 16 mL) was quickly injected into the solution, immediately followed by shaking until the solution turned dark red. The seed solution was refrigerated for 3–6 d before use. To make the K-Gold plating solution, 28 mg of potassium carbonate (K_2CO_3) was stirred in 100 mL water for 10 min. $HAuCl_4$ (25 mM, 1.5 mL) was added while stirring, and the solution with adjusted to pH 8–9 with dilute (~0.1 M) hydrochloric acid (HCl) or NaOH. The solution was refrigerated in darkness for 3–6 d before use.

2.2.2 Commercially Available Fe3O4 Nanospheres

A 6-mg/mL solution of nanoparticles in 0.7 mM CTAB was prepared and stirred for several hours to achieve good dispersion. NaOH (0.1 M, 0.4% volume/volume [v/v]) was added to the solution, followed by shaking for 30 min. Meanwhile, a TEOS solution (20% v/v in methanol) was prepared. The TEOS solution (0.9% v/v) was added to the nanoparticle solution, followed by shaking overnight. After purification several times, the nanoparticles were redispersed in ethanol. Ammonium hydroxide was added to the solution (40-µL/3-mL solution), which was then shaken for 10 min. APTES was added to the solution while sonicating (8-µL/1-mL solution) in 2 equal aliquots, with each addition followed by 30 min of sonication. The mixture was then shaken for 2 h, purified several times, and redispersed in water. Twice the volume of THPC seeds was added to the nanoparticle solution and, after being thoroughly mixed, it was refrigerated overnight. The nanoparticles were purified several times and redispersed in water. One milliliter of the nanoparticle solution was combined with 10 mL of K-Gold plating solution and vortexed for 1 min. A 38% formaldehyde solution (15 µL) was added and the solution was vortexed thoroughly, then shaken for 40 min. Finally, L-glutathione (15 µL) was added to stop the reaction, followed by thorough mixing. The nanoparticles were purified 3 times by centrifugation and dispersed in water. The nanoparticles were found to be weakly attracted to a strong magnet.

2.2.3 Magnetic Nanorods

The synthesis of silica-capped magnetic nanorods is based on methods published in literature.[25] A mixture of CTAB (1 g) and $FeCl_3 \cdot 6H_2O$ (1.08 g) was dissolved in 40 mL water and gently stirred at 80 °C for 12 h to form iron (III) oxide-hydroxide (FeOOH) nanorods. The reaction was accompanied by a color change from transparent gold to turbid orange. The nanorods were collected and purified by centrifuge 3 times and redispersed in water. To form silica-capped nanorods, PAA was added to the nanorods (3.33 mL for every 30 mg of nanorods in solution) and the mixture was stirred overnight at room temperature. The nanorods were collected and purified by centrifuge 3 times and redispersed in 3 mL of water. Assembly of a silica (SiO_2) shell on the FeOOH nanorods was achieved through the addition of stock 30% ammonium hydroxide (1 mL) under agitation, followed by the addition of ethanol (20 mL) and TEOS (60 µL), with the final solution being stirred for 1 h. The nanorods were collected and purified by centrifuge 3 times and dispersed in 2 mL of water.

To reduce the FeOOH to magnetic Fe_3O_4, 1 mL of the nanorods was sonicated with 15 mL of ethylene glycol for 3 min to disperse the nanorods. The solution was heated at 210 °C for 12 h in a Teflon-lined, stainless-steel hydrothermal vessel, then returned to room temperature. Alternatively, the nanorods were heated to 220 °C for 24 h in diethylene glycol. The nanorods were purified 3 times in ethanol by centrifuge and dispersed in 2.5 mL of ethanol. ATPES (250 µL) was added and the solution was shaken overnight. Following several purifications and redispersion in water, the nanorods were combined with twice the volume of THPC seeds, shaken 1 h, and refrigerated overnight. The nanorods were purified several times and dispersed in 3 mL of water. To plate the magnetic nanorods, 1 mL of the nanorods solution was vortexed with 10 mL of K-Gold plating solution for 1 min. A 38% formaldehyde solution (15 µL) was added and the solution was vortexed thoroughly, then shaken for 40 min. Finally, L-glutathione (15 µL) was added to stop the reaction, followed by thorough mixing. The nanorods were purified several times and dispersed in water. The nanorods produced were found to be intensely attracted to a strong magnet.

2.2.4 Synthesized Fe_3O_4

The synthesis of the Fe_3O_4 nanospheres was based upon literature.[26–28] $Fe(acac)_3$ (0.35 g, 1 mmol), 1,2-hexadecanediol (1.3g, 5 mmol), oleic acid (0.95 mL, 3 mmol), and oleylamine (1 mL, 3 mmol) were stirred in benzyl ether (10 mL) under flowing nitrogen (N_2). The solution was heated to 200 °C for 30 min, then to reflux (298 °C) for 30 min. After cooling, the solution was precipitated with ethanol, purified by centrifuge, and dispersed in hexanes. It was then heated to 100 °C for 30 min (to

remove hexanes), heated to 200 °C for 1 h, then refluxed (298 °C) for 1 h. After cooling to room temperature, the solution was again precipitated with ethanol, purified several times by centrifuge, and dispersed in hexanes.

To create the silica shell around the nanoparticles, Igepal-CO520 surfactant (5.17 mL) was sonicated in hexanes (87.5 mL) until well dispersed. To this solution, ammonium hydroxide (0.73 mL) and nanoparticle solution (5 mL of a 0.31-mg/mL solution in hexanes) were added and the mixture was shaken for 10 min. TEOS (0.5 mL or 0.5% v/v) was added and the solution was stirred overnight. Methanol was added to quench the reaction and the solids were purified several times by centrifuge and dispersed in ethanol to bring the volume to 100 mL.

To seed and plate the nanoparticles, ammonium hydroxide (1.33-mL or 40-μL/3-mL nanoparticle solution) was added and the mixture was shaken 10 min. The solution was allowed to sonicate, and during sonication APTES (400 μL or 20-μL/5-mL solution) was added and sonication continued for 30 min. After that time, an equal amount of ATPES was again added, followed by sonication for 30 more minutes. The solution was then purified by centrifuge and dispersed in water. The nanoparticle solution was combined with twice the volume of THPC seeds, shaken, and refrigerated overnight. The nanoparticles were purified several times by centrifuge and dispersed in water (70 mL). A 1:10 (v/v) solution of nanoparticle solution to K-Gold plating solution was made and vortexed to combine thoroughly. Formaldehyde solution (15 μL) was added and the solution was shaken vigorously until a color change was detected, followed by gentle shaking for 45 min. Finally, L-glutathione (15 μL) was added to stop the reaction, followed by thorough mixing. The nanoparticles were purified 3 times and dispersed in water. The nanoparticles produced were found to be intensely attracted to a strong magnet.

2.3 Characterization

Transmission electron microscopy (TEM) samples were prepared by the Langmuir–Schaefer technique. The gold nanorods (GNRs) were dispersed into chloroform and a small amount was carefully deposited on top of water in a vial. As the chloroform evaporated, the GNRs were able to self-assemble on the surface of the water; a TEM grid was then dipped onto the GNRs on water, parallel to the interface. TEM images were collected with a JEOL 2100 (Jeol, Peabody, MA) at 200 keV with an objective lens inserted. Scanning electron microscopy (SEM) and X-ray photoelectron spectroscopy (XPS) samples were prepared by drop-casting the nanoparticle solution onto silicon (Si) wafers that were rinsed twice with ethanol, isopropyl alcohol, and water followed by drying under N_2 gas. The solvent was allowed to evaporate and the samples were analyzed. Ultraviolet-visible

(UV-vis) measurements were taken with a Perkin Elmer UV-vis–near-infrared spectrophotometer operating over a range of 400 to 1200 nm, with a path length of 1 cm.

3. Results

3.1 Formation of Plasmonic Core-Shell Nanoparticles

UV-vis spectroscopy was utilized to confirm the presence of the Au seeds and plating on the nanoparticles. Figure 1 shows the absorption spectra obtained of the core-shell nanoparticles following attachment of the THPC seeds. Gold plating for both the commercially available magnetic iron oxide nanoparticles and the synthesized iron oxide nanoparticles was performed. In both cases, a distinct plasmonic peak is identified within the 500–600-nm wavelength region, consistent with the presence of a gold plasmon on the prepared core substrate. The peak observed for the seeded nanoparticles occurs at a slightly blue-shifted wavelength than that for the plated particles, which is due to the transition from a confined spherical plasmon to an asymmetric gold-shell structure.[29]

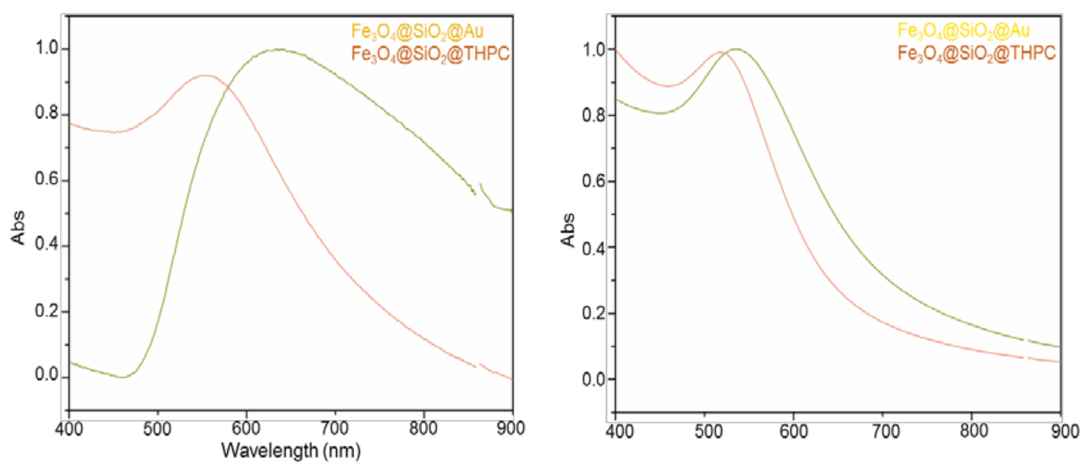

Fig. 1 UV-vis spectrum of gold-seeded (orange) and gold-coated (yellow) silica–iron oxide core-shell nanoparticles produced with commercially available (left) or synthesized (right) iron oxide nanoparticles as the magnetic core

UV-vis spectroscopy was performed following every step of the synthesis process for the core-shell magnetic nanorods; the results are displayed in Fig. 2. The characteristic plasmonic peak mentioned previously is absent from the spectra for the FeOOH nanorods, both before (black) and after (dark red) addition of the silica shell, as well as after hydrothermal treatment to reduce the nanorods to the ferromagnetic Fe_3O_4 species (red). It is noticeably present on the plated nanorods (yellow), indicating successful plating of the nanorods. Although the peak was

observed for the seeded nanospheres in Fig. 1, it is absent on the seeded nanorods. This absence might be a result of low surface coverage of the seeds on the nanorod surfaces (which is corroborated in Section 3.2).

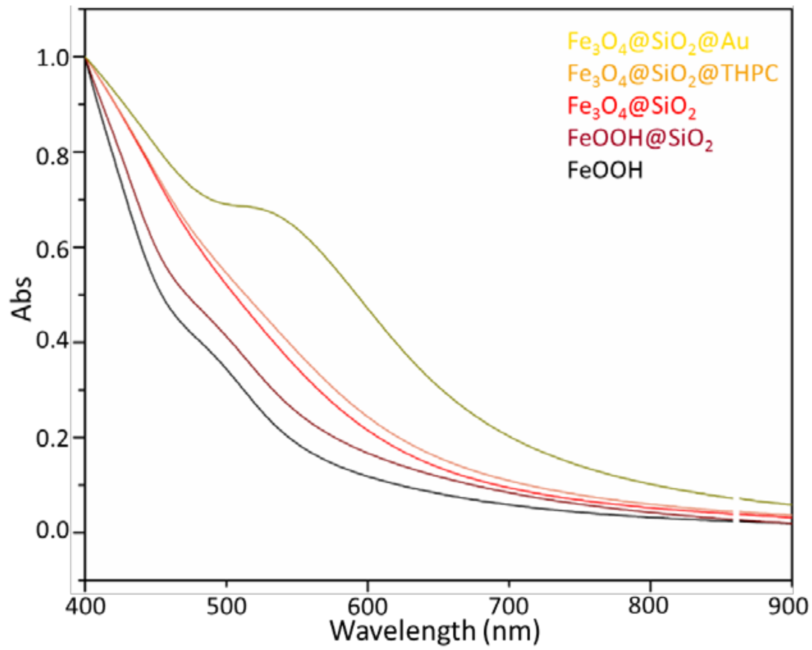

Fig. 2 UV-vis spectra of silica–iron oxide core-shell nanorods synthesized using hydrothermal conversion of FeOOH to magnetic iron oxide

While UV-vis spectroscopy indicates successful application of the THPC seeds and gold plating upon the nanoparticles, it does not indicate whether a uniform core-shell structure was successfully formed. For this, XPS was used to compare the surfaces of the nanoparticles after each step of the procedure. The survey spectra for the nanorods, displayed in Fig. 3, show the presence of the elemental species expected to be present on the nanoparticle surface. Peaks in the carbon (C) *1*s and oxygen (O) *1*s, as well as Si *2*s and *2*p, iron (Fe) *2*p, and Au *4*f and *4*d regions can be observed on many, if not all, of the spectra. In general, the spectra are similar to one another and there is an absence of extraneous peaks. A closer look at the key regions within these spectra is presented in Fig. 4.

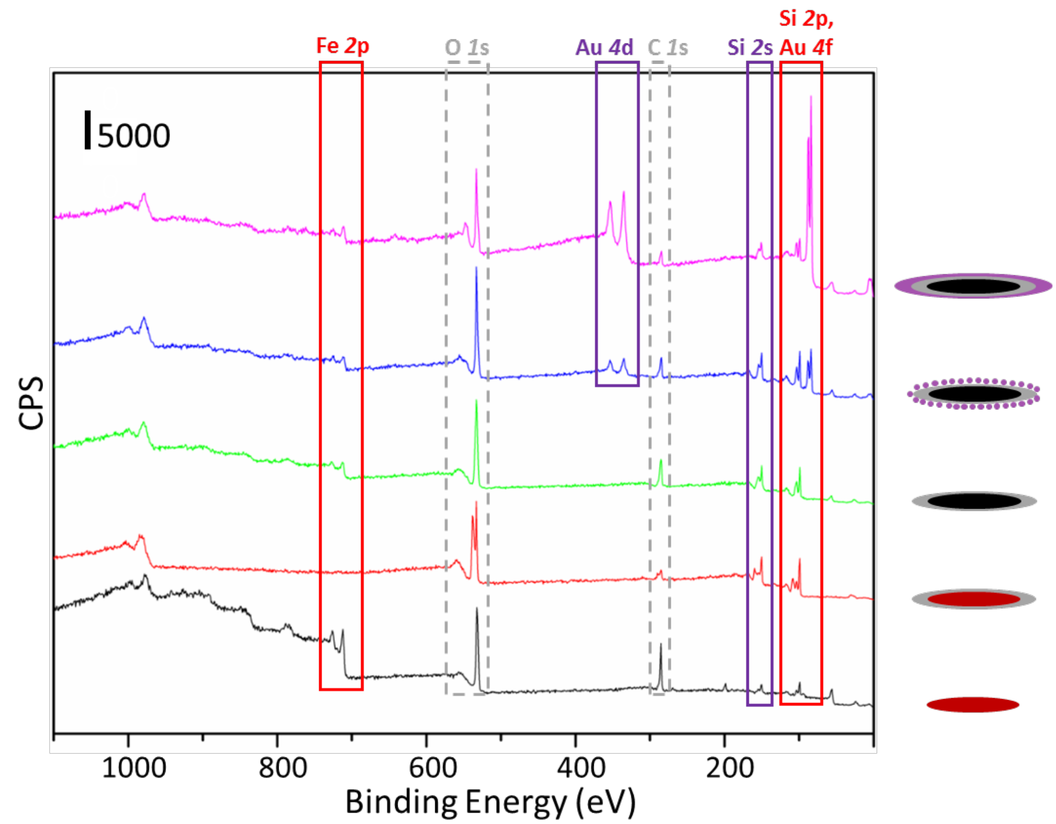

Fig. 3 XPS survey spectra for the nanorods during each step of the synthesis process

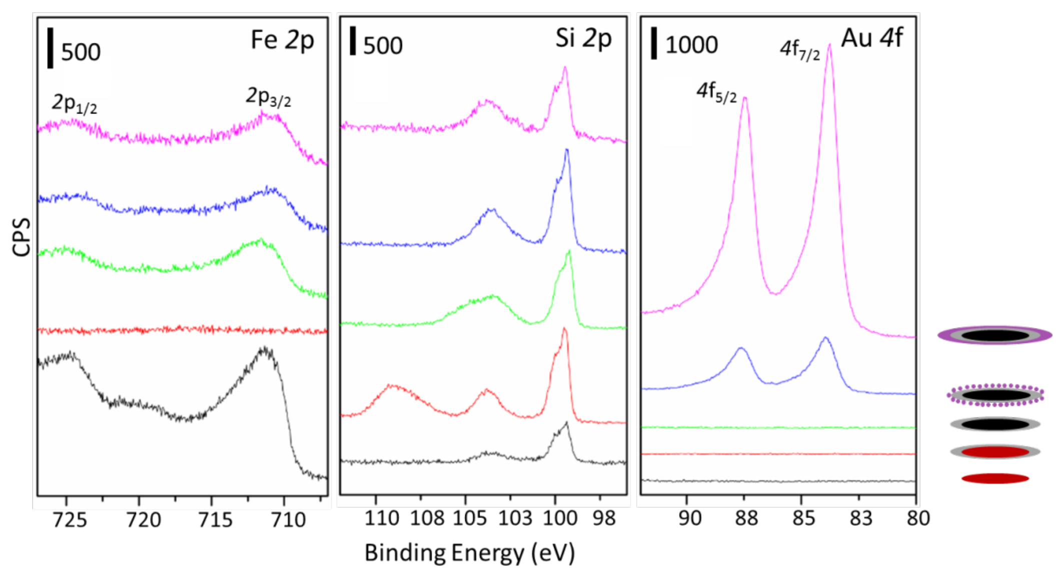

Fig. 4 Key regions within the XPS spectra of the nanorods during each step of the synthesis process

The left, middle, and right panels of Fig. 4 display the Fe *2*p, Si *2*p, and Au *4*f regions, respectively, of the XPS spectra. In all panels, the black spectrum represents the FeOOH nanorods, the red spectrum represents the silica-coated FeOOH nanorods, the green spectrum represents the silica-coated nanorods following hydrothermal conversion of the FeOOH core to magnetic Fe_3O_4, the blue spectrum represents the seeded core-shell nanorods, and the pink spectrum represents the gold-plated core-shell nanorods. The FeOOH nanorods themselves produce a strong signal in the Fe *2*p region with a possible satellite shake-up peak around 720 eV, indicative of Fe (III) oxide.[30] This signal is greatly reduced following the addition of the silica shell, hydrothermal reduction, and gold seeding and plating, which indicates the silica and gold layers are thin enough to permit the detection of electrons from the nanoparticle's core or, more likely, incomplete coverage of the iron oxide. A small signal is detected in the Si *2*p region for the FeOOH nanorods, which may be explained by the fact that the nanorods were dropcast and dried upon an Si wafer for XPS analysis. Following the addition of a silica shell, the intensity of the metallic and oxidized Si peaks within the Si *2*p region is increased for all samples compared to the bare nanorods. No gold is detected on the nanorods prior to addition of the THPC seeds, as is expected. The presence of Au *4*f species is clear on the seeded nanorods and the intensity is greatly increased for the gold-plated nanorods.

The XPS survey spectra (Fig. 5) obtained for the commercially available magnetic nanoparticles generally are in agreement with those for nanorods with the appearance of peaks indicating the presence of Si, following the formation of the silica shell, and gold, following the seeded and plating processes. The major difference is the absence of any Fe peaks, which may be due a thicker silica shell in the cases of the core-shell nanoparticles or from incomplete shell formation on the rod structure. The absence of Fe for the bare nanoparticles is attributed to oxide contamination and adventitious carbon on the nanoparticles' surface due to long-term storage of the nanopowder prior to its use here.

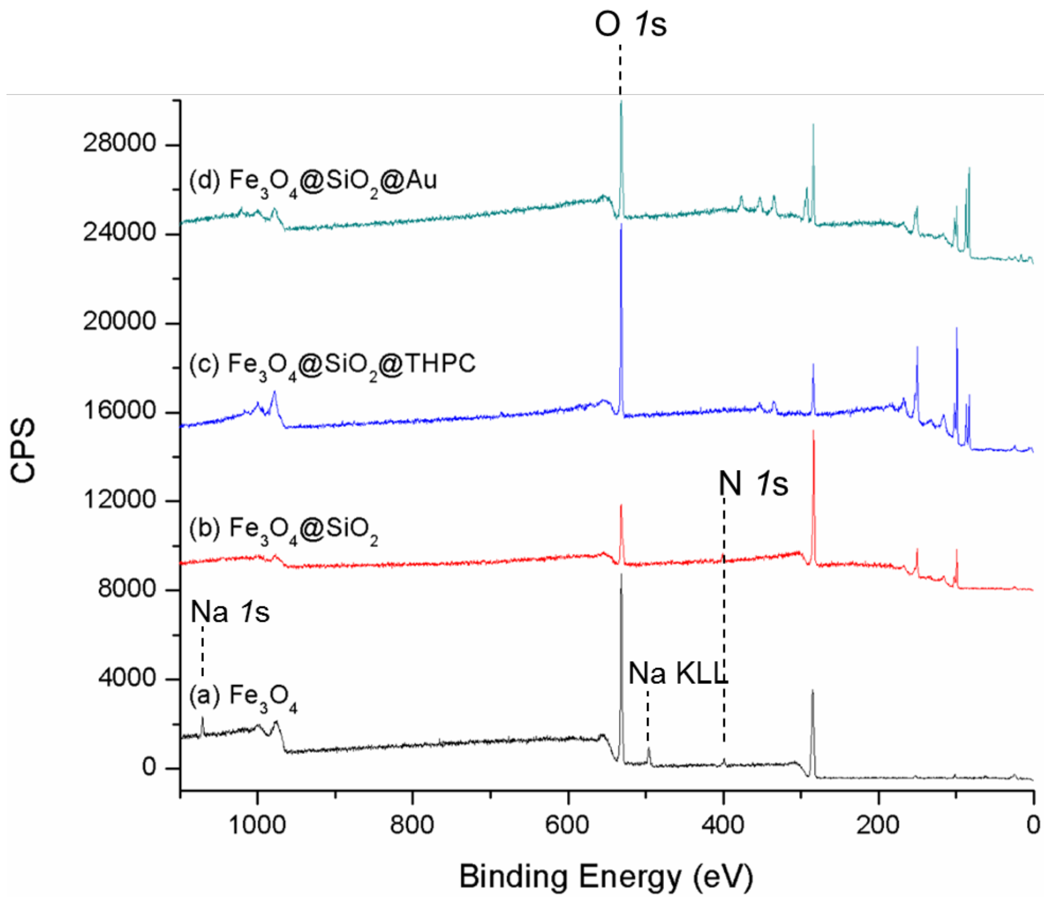

Fig. 5 XPS survey spectra for the commercially available nanospheres during each step of the silica-coating and gold-plating process

3.2 Preservation of Size and Shape

In the case of the nanorods, the XPS spectra are in agreement with successful plating of core-shell nanoparticles. Similar trends are found in the spectra for the commercially available nanoparticles. These results suggest the formation of magnetic core-shell nanoparticles is attainable using multiple pathways to result in tailored particles with specific magnetic strengths and desired geometries depending on the targeted application. This last point is very important for certain applications since the shape of the gold-plated nanoparticles will affect the optical properties of the material.[31] SEM and TEM were used to demonstrate that the procedure for forming these nanoparticles does not alter their geometry.

Figure 6 summarizes these images for the nanorods. The SEM and TEM micrographs of the FeOOH nanorods in Figs. 6a and 6b, respectively, show particles ranging about 200–300 nm in length and 50–100 nm in width, and are consistent with one another. After forming the core-shell structure and hydrothermal reduction to magnetic iron oxide, the silica-capped particles maintain

their size and shape, as seen in the SEM image in Fig. 6c. TEM was not performed on any of the magnetic materials. SEM micrographs of the seeded and gold-plated nanorods can be observed in Figs. 6d and 6e, respectively. These also show that the nanorods are able to maintain their original shape and size through the capping and plating process. Furthermore, the presence of the gold plating is confirmed in Fig. 6e, which supports previous XPS and UV-vis data and confirms the gold coverage on the nanorods' surface is incomplete, which may help explain the detection of the Fe *2*p signal on these samples in XPS. Gold and silica coverage on the magnetic nanorods could be improved by optimizing the concentrations of reagents used during the procedure. Despite this, microscopy techniques clearly indicate the general nanoparticle morphology and size remain unaltered throughout the process.

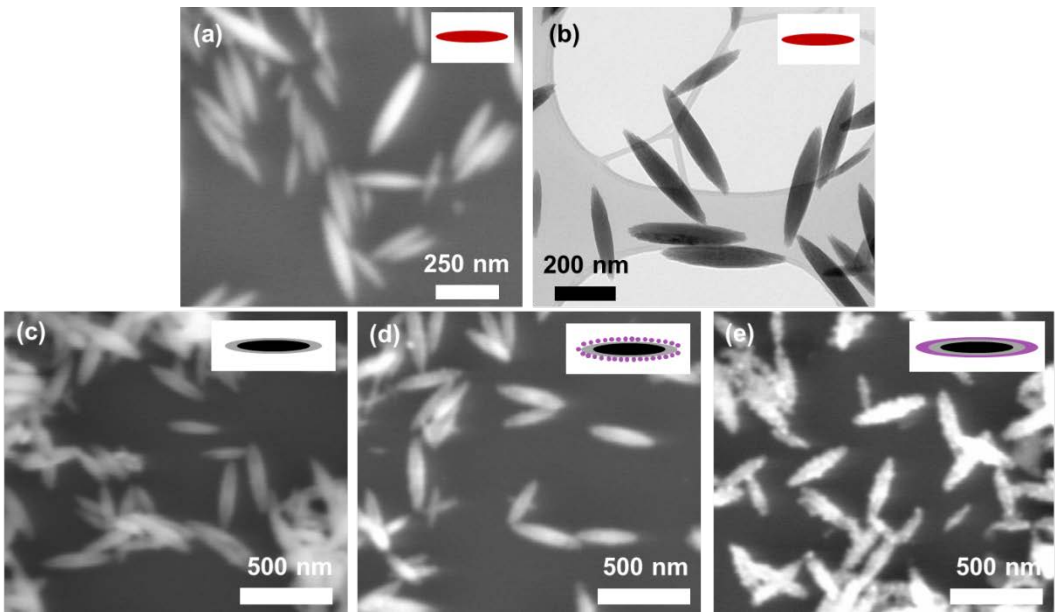

Fig. 6 SEM (a, c–e) and TEM (b) images of nanorods during each step of the silica-coating and gold-plating process

Three procedures were used to produce plasmonic magnetic core-shell nanoparticles of different shapes and varying degrees of magnetism. In all cases, the plasmonic peak from the gold was detected on the plated samples in UV-vis spectroscopy. XPS spectra throughout the synthesis process agree with successful silica capping and gold plating of the nanoparticles and microscopy techniques demonstrate the original nanoparticles' size and shape are preserved throughout the process.

4. Conclusions

In this work we demonstrated a new methodology to create asymmetric magnetic nanorods with a plasmonically active gold outer shell. The multistage approach

involves the synthesis of a precursor FeOOH nanorod, where the incorporation of a protective silica shell allows for the material/morphology to survive hydrothermal treatment and subsequent transition to magnetically responsive Fe_3O_4. On the magnetic nanorod–SiO_2 particle, a thin gold layer is grown to directly introduce tailorable plasmonic properties. This approach is demonstrated to be applicable to both spherical and asymmetric morphologies, allowing the hybrid materials to be readily engineered for precise magnetic and plasmonic responses.

5. References

1. Nguyen TD, Tran TH. Multicomponent nanoarchitectures for the design of optical sensing and diagnostic tools. RSC Adv. 2014;4(2):916–942.
2. Song EQ, Hu J, Wen CY, Tian ZQ, Yu X, Zhang ZL, Shi YB, Pang DW. Fluorescent-magnetic-biotargeting multifunctional nanobioprobes for detecting and isolating multiple types of tumor cells. ACS Nano. 2011;5 (2):761–770.
3. Zhang W, Suhr J, Koratkar N. Carbon nanotube/polycarbonate composites as multifunctional strain sensors. J Nanosci Nanotech. 2006;6(4):960–964.
4. Eswaraiah V, Balasubramaniam K, Ramaprabhu S. Functionalized graphene reinforced thermoplastic nanocomposites as strain sensors in structural health monitoring. J Mat Chem. 2011;21(34):12626–12628.
5. Grande L, Chundi VT, Wei D, Bower C, Andrew P, Ryhänen T. Graphene for energy harvesting/storage devices and printed electronics. Particuology. 2012; 10(1):1–8.
6. Bae J, Park YJ, Lee M, Cha SN, Choi YJ, Lee CS, Kim JM, Wang ZL. Single-fiber-based hybridization of energy converters and storage units using graphene as electrodes. Adv Mat. 2011;23 (30):3446–3449.
7. Boyne DA, Chipara AC, Griep MH. Transverse axis morphological control for tailored gold nanorod (GNR) synthesis. RSC Adv. 2016;6 (68):63634–63641.
8. Boyne DA, Griep MH., Decorated core-shell architectures: influence of the dimensional properties on hybrid resonances. Plasmonics. 2017;1–8.
9. Ali MRK, Wu Y, Tang Y, Xiao H, Chen K, Han T, Fang N, Wu R, El-Sayed MA. Targeting cancer cell integrins using gold nanorods in photothermal therapy inhibits migration through affecting cytoskeletal proteins. Proc Nat Acad Sci. 2017;114(28):E5655–E5663.
10. Paulo PMR, Zijlstra P, Orrit M, Garcia-Fernandez E, Pace TCS, Viana AS, Costa SMB. Tip-specific functionalization of gold nanorods for plasmonic biosensing: effect of linker chain length. Langmuir. 2017;33(26):6503–6510.

11. Shang W, Zeng C, Du Y, Hui H, Liang X, Chi C, Wang K, Wang Z, Tian J. Core–shell gold nanorod@metal–organic framework nanoprobes for multimodality diagnosis of glioma. Adv Mat. 2017;29(3):1604381.

12. Parida S, Maiti C, Rajesh Y, Dey KK, Pal I, Parekh A, Patra R, Dhara D, Dutta PK, Mandal M. Gold nanorod embedded reduction responsive block copolymer micelle-triggered drug delivery combined with photothermal ablation for targeted cancer therapy. Biochimica et Biophysica Acta (BBA)–Gen Sub. 2017;1861(1):3039–3052.

13. Ding T, Mertens J, Lombardi A, Scherman OA, Baumberg JJ. Light-directed tuning of plasmon resonances via plasmon-induced polymerization using hot electrons. ACS Phot. 2017;4(6):1453–1458.

14. Mirshahghassemi S, Ebner AD, Cai B, Lead JR, Application of high gradient magnetic separation for oil remediation using polymer-coated magnetic nanoparticles. Sep Pur Tech. 2017;179:328–334.

15. Wang Z, Qiao R, Tang N, Lu Z, Wang H, Zhang Z, Xue X, Huang Z, Zhang S, Zhang G, et al. Active targeting theranostic iron oxide nanoparticles for MRI and magnetic resonance-guided focused ultrasound ablation of lung cancer. Biomaterials. 2017;127:25–35.

16. Wang F, Yang Y, Ling Y, Liu J, Cai X, Zhou X, Tang X, Liang B, Chen Y, Chen H, et al. Injectable and thermally contractible hydroxypropyl methyl cellulose/Fe3O4 for magnetic hyperthermia ablation of tumors. Biomaterials. 2017;128:84–93.

17. Joanna W, Jeremy P, Alexander S. Magnetic nanoparticles: new perspectives in drug delivery. Curr Pharm Design. 2017;23:1–10.

18. Kang T, Li F, Baik S, Shao W, Ling D, Hyeon T. Surface design of magnetic nanoparticles for stimuli-responsive cancer imaging and therapy. Biomaterials. 2017;136:98–114.

19. Choi JS, Kim S, Yoo D, Shin TH, Kim H, Gomes MD, Kim SH, Pines A, Cheon J. Distance-dependent magnetic resonance tuning as a versatile MRI sensing platform for biological targets. Nat Mater. 2017;16(5):537–542.

20. Canet-Ferrer J, Albella P, Ribera A, Usagre JV, Maier SA. Hybrid magnetite-gold nanoparticles as bifunctional magnetic-plasmonic systems: three representative cases. Nano Horiz. 2017;2(4):205–216.

21. Luo Z, Wang Y, Lu X, Chen J, Wei F, Huang Z, Zhou C, Duan Y. Fluorescent aptasensor for antibiotic detection using magnetic bead composites coated with

gold nanoparticles and a nicking enzyme. Analytica Chimica Acta. 2017;984:177–184.

22. Sood A, Arora V, Shah J, Kotnala RK, Jain TK. Multifunctional gold coated iron oxide core-shell nanoparticles stabilized using thiolated sodium alginate for biomedical applications. Mat Sci Eng: C. 2017;80:274–281.

23. Hu R, Zheng M, Wu J, Li C, Shen D, Yang D, Li L, Ge M, Chang Z, Dong W. Core-shell magnetic gold nanoparticles for magnetic field-enhanced radio-photothermal therapy in cervical cancer. Nanomaterials 2017;7(5):111.

24. Monaco I, Arena F, Biffi S, Locatelli E, Bortot B, La Cava F, Marini GM, Severini GM, Terreno E, Franchini CM. Synthesis of lipophilic core–shell Fe3O4@SiO2@Au nanoparticles and polymeric entrapment into nanomicelles: a novel nanosystem for in vivo active targeting and magnetic resonance–photoacoustic dual imaging. Biocon Chem. 2017;28(5):1382–1390.

25. Wang M, Gao C, He L, Lu Q, Zhang J, Tang C, Zorba S, Yin Y. Magnetic tuning of plasmonic excitation of gold nanorods. J Amer Chem Soc. 2013;135(41):15302–15305.

26. Zhang L, He R, Gu HC. Oleic acid coating on the monodisperse magnetite nanoparticles. App Sur Sci. 2006;253(5):2611–2617.

27. Lien YH, Wu TM. Preparation and characterization of thermosensitive polymers grafted onto silica-coated iron oxide nanoparticles. J Coll Inter Sci. 2008;326(2):517–521.

28. Ming Z, Brian LC, Charles JOC. Synthesis and characterization of monodisperse ultra-thin silica-coated magnetic nanoparticles. Nanotechnology. 2008;19(8):085601.

29. Boyne DA, Griep MH. Decorated core-shell architectures: influence of the dimensional properties on hybrid resonances. Plasmonics. 2017 Jun.

30. Muhler M, Schlögl R, Ertl G. The nature of the iron oxide-based catalyst for dehydrogenation of ethylbenzene to styrene 2. Surface chemistry of the active phase. J Catal. 1992;138(2):413–444.

31. Mackenzie GW, Devon AB, Mark HG. Rapid synthesis of high purity gold nanorods via microwave irradiation. Mat Res Exp. 2017;4(3):035040.

List of Symbols, Acronyms, and Abbreviations

APTES	(3-aminopropyl)triethoxysilane
Au	gold
C	carbon
CTAB	cetyltrimethylammonium bromide
Fe	iron
$Fe(acac)_3$	iron (III) acetylacetonate
$FeCl_3 \bullet 6H_2O$	iron (III) chloride hexahydrate
Fe_3O_4	iron (II, III) oxide
FeOOH	iron (III) oxide-hydroxide
GNR	gold nanorod
$HAuCl_4$	chloroauric acid
HCl	hydrochloric acid
K_2CO_3	potassium carbonate
N_2	nitrogen
NaOH	sodium hydroxide
O	oxygen
PAA	polyacrylic acid sodium salt
SEM	scanning electron microscopy
Si	silicon
SiO_2	silicon dioxide
TEM	transmission electron microscopy
TEOS	tetraethoxy orthosilicate
THPC	tetrakis(hydroxymethyl)phosphonium chloride
UV-vis	ultraviolet-visible

v/v	volume/volume
XPS	X-ray photoelectron spectroscopy

1 (PDF)	DEFENSE TECHNICAL INFORMATION CTR DTIC OCA
2 (PDF)	DIR ARL IMAL HRA RECORDS MGMT RDRL DCL TECH LIB
1 (PDF)	GOVT PRINTG OFC A MALHOTRA
4 (PDF)	DIR USARL RDRL WMM A J SANDS E WETZEL A BUJANDA M GRIEP